PERFORATION OF PLATES THROUGH HIGH-VELOCITY IMPACT

L. A. Merzhievskii and V. M. Titov

UDC 629.198.624

Presented are the results of an experimental investigation of the process of deformation of a body as it impacts and perforates thin plates, the impact speeds being in the range from 3 to 9 km/sec. We show that in a first approximation the radial deformation rate of the body is proportional to the mass velocity determined from the impact parameters; we also show that the initial stage of the process can, with sufficient accuracy, be described within the framework of the simplest hydrodynamic models. We establish the fact that the body debris particles have sizes distributed in accordance with the Rosen–Rammler law and we show that the ratio of the maximum velocity of these particles to the impact velocity is a function of the geometrical dimensions and densities of the body and target.

Interest in the phenomenon of the perforation of a plate by a particle impacting it at speeds ranging from 1 to 10 km/sec is primarily associated with the problem of how to protect space vehicles against the impact of a meteoroid by using a shield, i.e., a plate placed in front of the space vehicle, the thickness of this plate being less than the perforation limit thickness of the structure being protected. Numerical calculations given in [2], based on a hydrodynamic model of this phenomenon, present a picture of the initial stage of the process of interation of the body with the plate. A description of the process based on such a model does not permit an analysis of the debris field behind the shield. An analysis of this kind is particularly important when the spacing between the shield and the structure being shielded, i.e., the target, is large; in this case, the blow to the structure results from individual debris concentrations. Owing to boundary effects, discrete debris fragments appear behind the shield even when the maximum increase in the internal energy behind the front of the shock wave in the body and the shield considerably exceeds the heats of vaporization of the materials involved. A solution of the problem, which takes into account strength properties and failure characteristics of the materials in the presence of a high deformation rate, is not available, even in the simplest case when the shield thickness is small in comparison with the size of the impacting body. It is therefore natural to treat these problems experimentally. Experimental data retain their significance even for the purpose of making approximate engineering estimates in the initial stage of deformation of the body.

In the present paper we present the results of an investigation of the impact process on the basis of experiments conducted with impact speeds in the range from 3 to 9 km/sec. Steel spheres with a diameter of 2.5 mm were accelerated by means of an explosive shaped-charge accelerator (see [3]). Plates of steel and Duralumin of thickness varying from 1 to 3 mm were accelerated by explosive means, as were also bodies of cylindrical shape with height equal to the diameter (4 mm). The method of projection in this case is close to that described in [4]. For realizing much higher velocities at impact we also employed a method in which a plate and a body were simultaneously projected toward each other. The study of the initial stage of the deformation process in the body was made with the aid of flash x-ray pictures; this was done in the case of the projection of a flat plate onto a large fixed cylindrically shaped body (usually 10 × 10 mm). The plate parameters are given in Table 1.

TABLE 1

Plate material	δ, mm	v_0, km/sec
Steel	1	4,6±0,15
»	1	3,95±0,15
»	2	3,9±0,15
Aluminum	2	5,1±0,15

Novosibirsk. Translated from Zhurnal Prikladnoi Mekhaniki i Tekhnicheskoi Fiziki, No. 5, pp. 102–110, September-October, 1975. Original article submitted August 7, 1974.

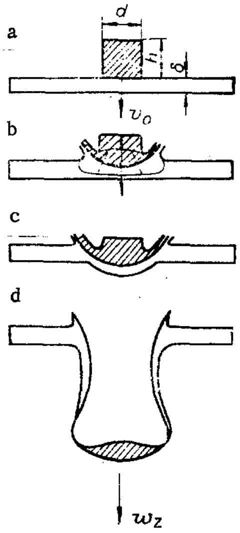

Fig. 1

1. We consider high-speed impact at speed v_0 of a cylinder of height h and diameter d (where h is close to d) onto a plate of thickness δ (see Fig. 1a); the densities of the cylinder and of the plate are, respectively, ρ_0 and ρ_1. At the instant of impact shock waves begin to propagate into the cylinder and the plate (these are indicated by arrows in Fig. 1b). A rarefaction waves arises at the lateral surface of the cylinder, causing the material to spread out (shown shaded). After the shock wave exits at the rear surface of the plate a centered rarefaction wave propagates backward into its interior and the material then begins to flow (Fig. 1c). At a definite stage (see Fig. 1d) the plate material is deformed with the residual body material into a shroud, which upon rupture results in a field of debris fragments.

The simplest case to treat is the case of a thin plate ($h \gg \delta$). The problem is then reduced to considering deformation of a body as the result of passage through it of a shock wave of given strength and duration. A study of the impact-induced processes taking place in the body can be made based on experimental data relating to planar shock waves in metals [2, 4]. From a knowledge of the pertinent shock adiabats one can obtain, corresponding to a specified impact speed v_0, the mass velocity u_p behind the shock front (when the materials of the impacting bodies are alike, $u_p = v_0/2$), the speed of the front u_s, the compression $\gamma = \rho_*/\rho_0$ (ρ_* is the density behind the front), and the pressure $p = \rho_0 u_p u_s$. Recall that we are dealing here with the "reverse" situation, namely, the impact of the plate on the body.

The rarefaction wave, originating at the rear surface of the plate, overtakes the front of the shock wave moving in the body at a distance into the body given by

$$l = \frac{1/u_s' + 1/\gamma c'}{1/u_s - 1/\gamma c}\delta,$$

where c is the velocity of sound behind the front; the primes refer to the corresponding parameters for the plate (they apply when the plate and body materials are not alike). In the experiments reported here (see Table 1) the value of l varied from h/2 to h.

In relieving the pressure arising at impact an essential role is also played by the rarefaction wave emanating from the lateral free surface of the cylindrical body. The distance into the body at which the shock front, as yet unaffected by the action of unloading from the rear surface of the plate, is first attenuated by this lateral rarefaction wave is given by

$$l_1 = d/2\,\mathrm{tg}\,\alpha,$$
$$\mathrm{tg}\,\alpha = \left[(c/u_s)^2 - (u_s - u_p)^2/u_s^2\right]^{1/2},$$

where α is the lateral unloading angle. In the case of strong shocks, $\tan\alpha \simeq 0.7$ over a wide range of pressures and for varying materials, i.e., $l_1 \simeq 0.7d$ (see [4]).

In [2] the assumption was made that for the purpose of making engineering estimates a one-dimensional model of the impact process could be used. Simple experiments show, however, the substantial role played by the lateral rarefaction wave when $h \simeq d$. To verify this, we recorded the axial speed v_1 of a steel foil of thickness $\delta = 0.3$ mm, placed at the rear end face of steel cylinders of height h = 10 mm and of diameters d = 10 mm and d = 30 mm (these were impacted by a steel plate of thickness $\delta = 1$ mm at a speed of $v_0 = 4.6$ km/sec). For the case d = 10 mm the shock front was attenuated by the lateral rarefaction wave; for the case d = 30 mm, a zone of about 15 mm was unaffected by this wave; in each case the unloading conditions from the rear free surface of the plate remained constant. The results are shown in Table 2; they show a sharp difference in the values of v_1; in view of the small data base the experimental errors are large, but not, however, greater than 15%. The values of p and u_p given here are those corresponding to the instant of impact at the boundary between the plate and the body. In the one-dimensional case the value of v_1 is close to twice the value of the maximum mass velocity at the end face; it is evident from Table 2 that there is a noticeable drop in the mass velocity (and in the pressure) over the path h, i.e., after a characteristic time for the wave processes, namely, $t_s \sim h/u_s$ (in order of magnitude).

TABLE 2

h, mm	d, mm	p, Mbar	u_p, km/sec	v_1, km/sec
10	10	1.4	2.3	0.86
10	30	1.4	2.3	1.9

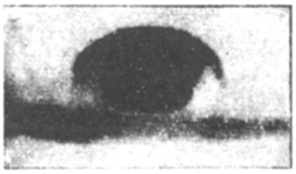

Fig. 2

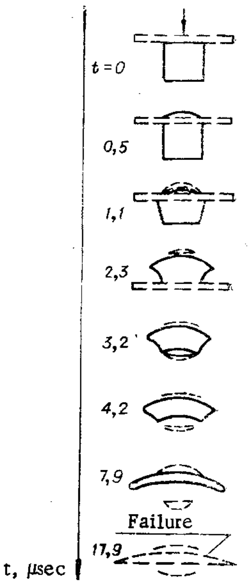

Fig. 3

Figure 2 shows an x-ray photograph of a deforming specimen of lead 2.7 μsec after being impacted at v_0 = 5.1 km/sec by an aluminum plate of thickness δ = 2 mm. Figure 3 indicates at successive time instants the deformation process occurring in a steel body impacted at v_0 = 3.9 km/sec by a steel plate of thickness δ = 2 mm (as deduced from flash x-ray pictures). In our work we used a 4-framing apparatus, so that in a given series of time-frames an error of $\Delta t \simeq 0.2$ μsec is possible in the various experiments. The dashed configurations define the spalls and delaminations which occur at the free surfaces. Total failure of the body was recorded at a time of $T \simeq 18$ μsec (crack formation is possible at a much earlier time), i.e., the time to complete rupture $T \gg t_s$ (here u_s = 7.1 km/sec). In view of the above, we can say that, in the main the deformation process takes place at a constant density ρ_0, i.e., we can consider this process within the framework of a model of an incompressible medium. Similar conclusions can be made in analyzing the deformations of bodies of other material compositions.

Initial conditions for the inertial flow are determined by the field of velocities created in the body during the interaction of the shock wave with the rarefaction waves. In analyzing the data of Table 2, we remarked that the value of the mass velocity at the rear end face of the body was much less than u_p. The flash x-ray photographs make it possible to record the displacement of the opposite ("working") end of the body and to determine its speed $\tilde{u}_p(t)$ (particularly in the case involving aluminum plates); however, this can only yield an order of magnitude estimate of $\tilde{u}_p$ in view of the natural diffuseness of the image on the x-ray plates. Such estimates show that for $t \sim t_s$ the value of $\tilde{u}_p$ is still about $\sim 0.5\, u_p$; they also show that the form of the decreasing function $\tilde{u}_p/u_p = f(t)$ is similar for bodies of various materials.

More reliable information is given by a measure of the maximum radius r (t) of the deforming body, although its determination is connected with an unavoidable error (see Fig. 2). The results of measuring $w_r = dr/dt$ for t = 5 μsec (which amounts to from 3 to 4 t_s) are shown, in terms of u_p, w_r, in Fig. 4 (the body here is steel and the impacting plates, listed according to material, thickness, and impact velocity, are as follows: 1) aluminum, δ = 2 mm, v_0 = 5.1 km/sec; 2) steel, δ = 2 mm, v_0 = 3.9 km/sec; 3) steel, δ = 1 mm, v_0 = 3.95 km/sec; 4) steel, δ = 1 mm, v_0 = 4.6 km/sec; the other body–plate combinations represented in this figure are as follows: aluminum body and aluminum plate (5) with δ = 2 mm, v_0 = 5.1 km/sec; tungsten body (a collection of plates) and a steel plate (6) with δ = 1 mm, v_0 = 4.6 km/sec; lead body and an aluminum plate (7) with δ = 2 mm, v_0 = 5.1 km/sec). The data show that for the various materials there is a unique relationship between the values of u_p and w_r, i.e., $w_r \simeq f(u_p)$ (as a rough approximation we can take $w_r \simeq ku_p + b$, where k and b are constants). We remark that for the dimensions in question the value of w_r stays practically constant when t > 5 μsec.

In the experiments conducted here the body materials had strengths varying over an order of 1.5-2 (from lead to steel). The influence of the strength characteristics in the description of the deformation of a body for $v_0 \gtrsim 4$ km/sec has not been remarked upon. There is thus the possibility of using this information to model the deformation process in terms of an incompressible fluid. It should be noted that the strength characteristics of a material can have a substantial influence on the size of the spall fragments that are formed in the final stage of the deformation process.

We consider the start of an inertial flow in a setting similar to that assumed in [5, 6] in calculating the initial stage of a directed explosion. Let the material of a cylinder of unit radius (h = d) consist of an ideal incompressible fluid, and let the boundary conditions be

$$v_z = \frac{\partial \varphi}{\partial z} = \quad \text{for} \quad z = 0, \tag{1.1}$$

$$\varphi = 0 \quad \text{for} \quad z = h,$$

$$\varphi = 0 \quad \text{for} \quad z = 1,$$

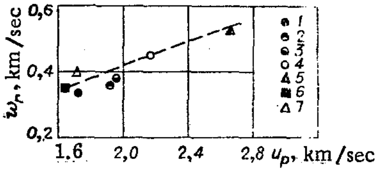

Fig. 4

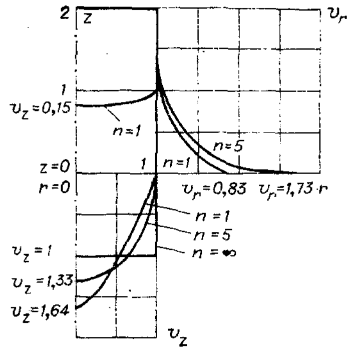

Fig. 5

where φ is the velocity potential and z and r are, respectively, the axial and radial coordinates. Physically, these conditions correspond to assigning the velocity on the base of the cylinder and setting the pressure equal to zero on the remaining surface of the cylinder. The solution of the equation

$$\frac{\partial^2\varphi}{\partial r^2} + \frac{1}{r}\frac{\partial\varphi}{\partial r} + \frac{\partial^2\varphi}{\partial z^2} = 0$$

subject to the conditions (1.1) has the form

$$\varphi = \sum_{i=1}^{\infty} \frac{J_0(p_i r)}{J_1(p_i)} \frac{\Phi_i}{p_i} \frac{\operatorname{sh} p_i(z-h)}{\operatorname{ch} p_i h},$$

where the p_i are the zeros of the Bessel function of order zero, J_0, i.e., $J_0(p_i) = 0$, $\Phi_i = J_i(p_i)/p_i$ (J_1 is the Bessel function of the first order). Then

$$v_z = \frac{\partial\varphi}{\partial z} = 2\sum_{i=1}^{\infty} \frac{J_0(p_i r)}{p_i J_1(p_i)} \frac{\operatorname{ch} p_i(z-h)}{\operatorname{ch} p_i h}, \qquad (1.2)$$

$$v_r = \frac{\partial\varphi}{\partial r} = -2\sum_{i=1}^{\infty} \frac{J_1(p_i r)}{p_i J_1(p_i)} \frac{\operatorname{sh} p_i(z-h)}{\operatorname{ch} p_i h}.$$

If we limit ourselves to the first terms of the series, this corresponds to a drop in the velocity towards the base periphery. The results obtained in computing the velocity field are shown in Fig. 5 for n = 1 and n = 5 (n is the number of terms); the values given here are those of $v_z(r)$ for z = 0 and z = 1; also displayed are the values of $v_z(z)$ for r = 1. When z = 2, the value of $v_z \simeq 0$. The value of v_r for z = 0 and r = 1 increases rapidly with increasing n (the series $\sum_{i=1}^{\infty} \frac{2}{p_i} \operatorname{th} 2p_i$, to which the series (1.2) reduces, is divergent). This is the analytical analog of the boundary shroud seen on the x-ray pictures. It can be confirmed that the order of magnitude of the velocity $v_r(z)$ corresponds to that observed in the experiments, wherein it was assumed that the maximum $v_z \sim 0.5u_p$ in agreement with the estimate indicated above.

The modelling considerations employed above assume that the material of the body is macroscopically continuous. Therefore, if the impact speed is very high (v_0 greater than 10 to 15 km/sec), these considerations are not applicable, since the material may begin to vaporize when unloading takes place behind the shock wave. The process becomes significantly more involved and does not admit of a simple analysis, even in the case when the plate thickness $\delta \gg h$, since then the flow of the plate material must also be considered.

2. Logically, it would be more satisfying to consider not the deformation process in the body, but rather to solve the complete problem involving the deformation of the body and its fragmentation into individual debris particles when it is subjected to a short duration shock impulse. However, to this time there exists no exact formulation for treating the problem concerned with the failure of a material; one reason for this is the lack of information concerning the physicomechanical properties of a material under the conditions existing when the body−target collision occurs. It is possible to obtain an approximate

TABLE 3

d, mm	v_0, km/sec	δ, mm	$E(x)$	$S(x)$	Δ_1	Δ_2	χ^2	μ_0
0.9	5,5	1	0,18	0,0219	0,0012	0,0002	2,7	0,51
0.9	5,5	0,5	0,255	0,052	0,0041	0,0007	3,1	0,487
0.83	7,5	0,1	0,15	0,0152	0,0008	0,00016	2,85	0,49

solution of the problem by statistically investigating the parameters of the debris cloud penetrating through the target. Since current experimental techniques make it impossible to record each individual fragment, an idea of the sizes of these fragments can be obtained by the dimensions of the cavities they make on a backup plate behind the target. A preliminary inspection of the available experimental data has shown that the cavity sizes are distributed in accordance with the Rosen–Rammler law (see [7])

$$V(x) = V_0 \exp\left[-(x/x_0)^m\right], \tag{2.1}$$

where V_0 is the sum of all the cavity dimensions of the cavities on the backup plate; $V(x)$ is the sum of the dimensions of all cavities with diameters larger than x; x_0 and m are constants determined in the experiments. To correctly verify this assertion one would need a quantitative indication of how well the hypothetical distribution function agrees with the overall experimental results. There are several such indicators available, each giving rise to a corresponding criterion for goodness of fit. We tested and verified the hypothesis advanced above with the aid of the much used χ^2 and Kolmogorov criteria. The values of the quantities χ^2 and μ_0, calculated from the experimental data, are shown in Table 3 (μ_0 is a parameter defining the extent to which hypothesis and experiment agree when the criterion being used is that due to Kolmogorov). It follows from the data obtained that the probability of agreement of the experimental data with the results predicted by the relation (2.1) is at least 95%, i.e., it is practically certain that the distribution of the dimensions of the cavities formed by the debris cloud from the target on the backup plate is described by the Rosen–Rammler law.

Let x_i, $i = 1, 2, 3, \ldots, N$, be a sample of experimental points (where x_i is the diameter of the i-th cavity and N is the number of cavities measured); let $E(x)$ and $S(x)$ be, respectively, the mathematical expectation and the dispersion of the random variable x. Approximately, we have

$$E(x) \simeq \frac{1}{N}\sum_{i=1}^{N} x_i, \quad S(x) \simeq \frac{1}{N}\sum_{i=1}^{N}(x_i - E(x))^2,$$

then, in seeking the parameters of the distribution (2.1), we can use the following relations established in [8], namely,

$$E(x) \simeq x_0, \quad S(x) \simeq \frac{x_0^2}{m}.$$

Values of the quantities $E(x)$ and $S(x)$ are given in Table 3 along with the 95% confidence limits (Δ_1 and Δ_2, respectively).

In adapting our relationships to the fragment dimensions we used the modelling curve given in [9]; we also used the fact that for experimentally achievable impact speeds the cavities created in the backup plate materials were close to spherical in form. The modelling curve, with good accuracy, may be described by the relation

$$\frac{L}{d_0} \simeq c_1 \ln \frac{\rho_0 v_0^2}{H_1}, \quad c_1 = \text{const},$$

where L is a cavity depth; H_1 is the dynamic hardness of the backup plate material. The data presented in Sec. 2, and the results given in [10], confirm the fact that the dispersion of velocities in the main mass of debris fragments is not large and can, in a first approximation, be neglected. Taking all these facts into account, we obtain

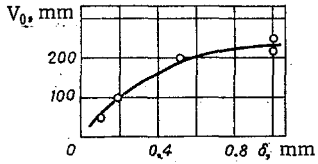

Fig. 6

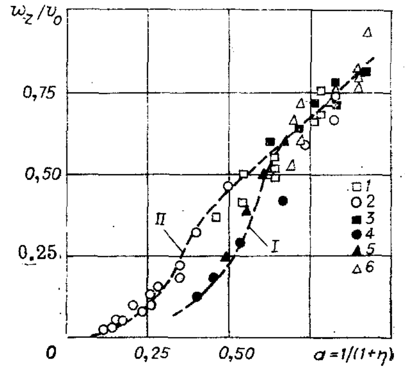

Fig. 7

$$\frac{x_i}{d_i} \simeq c_2, \quad c_2 = \text{const};$$

here d_i is the diameter of a fragment. We can now show that

$$V(d_i) = V_0 \exp\left[-\left(\frac{c_2 d_i}{x_0}\right)^m\right],$$

i.e., the distribution of fragment sizes also obeys the Rosen–Rammler law, and the parameters in the distributions for the fragments and the cavities are connected by means of obvious relationships. The value of V_0 varies depending on the conditions of the experiment. Figure 6 shows how V_0 depends on the plate thickness δ (impact speed v_0 = 5.5 km/sec, d_0 = 0.9 mm).

3. We return to the question concerning the velocity of the fragments penetrating beyond the perforated target (plate). In the experiments, the simplest procedure is to record the maximum velocity in a direction normal to the surface; this velocity, which we denote by w_z (see Fig. 1), will be referred to henceforth as the residual velocity (the fragment velocity beyond the perforated plate). Let the impacting body be a cylinder with $h \sim d$. It is obvious that for $h \gg d$ the value of w_z corresponds to the velocity of the center of mass of the deforming body, and, from general physical considerations, its value is close to the estimate obtained from momentum conservation, namely,

$$\frac{w_z}{v_0} \simeq \frac{1}{1+\eta}, \tag{3.1}$$

where $\eta = \delta\rho_1/h\rho_0$, i.e., the ratio of the masses of the target and the body per unit surface area.

If $h \sim \delta$, then, apart from residual effects associated with wave processes, a crude approximation may be had by taking the system of parameters defining the phenomena to be the following: w_z, v_0, ρ_0, ρ_1, δ, h, σ, where σ is a strength property of the target material. Then

$$\frac{w_z}{v_0} = f\left(\eta, \frac{\rho_0 v_0^2}{\sigma}, \frac{\rho_1}{\rho_0}\right) \tag{3.2}$$

(a more complete system of parameters (see [11]) can be written; however, its analysis in connection with the experimental results is rather involved). We consider below, for $h \lessdot \delta$, experimental results for specific pairs of materials: in particular, we consider the impact of a steel particle onto steel and aluminum targets. In each case, the dependence (3.2) is fairly strict, since all the remaining parameters, with the exception of η and $\rho_0 v_0^2/\sigma$, stay constant. Measurements of w_z were made with the aid of flash x-ray photographs of the dispersing debris cloud. In one group of experiments steel cylinders with h = 3.5 mm and d = 4 mm impacted plates of steel and aluminum. The experimental procedures varied: in some, bodies were projected end-on; in others, plates were projected into the bodies, and in still others, plates were projected toward one another simultaneously (in all cases, w_z was reckoned with respect to the plate). The accuracy in measuring w_z/v_0 was at least 10-12%. The velocities achieved experimentally varied from 3 to

8 km/sec for $\tilde{\delta} \le h$. A number of experiments of a similar type were made using bodies and plates of titanium and tungsten.

In a second series of experiments steel spheres, accelerated by means of an explosive shaped-charge accelerator, perforated targets of aluminum and steel. Target thickness were in the interval $d \le \delta \le \delta_0$ (δ_0 is the ballistic limit thickness of the target, (see [1]). The impact speed varied from 5 to 10 km/sec; d_0 varied from 0.75 to 2.3 mm; the accuracy in determining w_z/v_0 was at least 10%.

The experimental results are shown in Fig. 7, plotted, along with the data from [12], in terms of the coordinate variables w_z/v_0 and $a = 1/(1 + \eta)$ (the data 1 were for the impact of a steel cylinder onto a steel plate; data 2 were for the impact of a steel sphere onto a steel plate; data 3 involved the impact of an aluminum cylinder into a steel plate; data 4 involved the impact of an aluminum sphere onto a steel plate; data 5, taken from [12], were for the impact of an aluminum cylinder onto a steel plate; data 6 were for impacts involving other materials). Of the parameters defining the complete system of parameters, one is the body-shape parameter [in the relation (3.2) it was taken to be constant]. The experimental results show that, to within experimental error, the quantity w_z/v_0 is constant if one compares sphere and cylinder impacts onto a given target, the impacting bodies having the same mass. On the strength of this, we have, for a sphere, $\eta = \delta\rho_1/0.875\, d_0\rho_0$.

As can be seen from Fig. 7, when $h > \delta$ the relation (3.1) is obeyed satisfactorily (taking possible experimental error into account). A more accurate relationship is $w_z/v_0 \simeq k_1 a$, where $k_1 \simeq 0.9$ (the dashed line in Fig. 7). As δ increases, part of the momentum of the body begins to be absorbed by the target and the relation (3.1) then ceases to hold. The target thickness, for which a deviation from the relation (3.1) begins to be noticeable, is a function of the density of the target material. This can be seen from the data of Fig. 7 for steel and aluminum targets in the case of impact by a steel particle, where the curve I corresponds to impact onto aluminum and curve II, to impact onto steel. The difference in these curves is due essentially to the differing values of the parameters ρ_1/ρ_0 in the relation (3.2); it is connected physically with a change in the geometry of the interaction process with a change in the target density. It is to be expected that for much lighter materials the departure from a linear dependence will occur for large values of the parameter a. In the experiments with $a < 0.5$, we used steel targets of differing qualities, involving roughly a two-fold difference in strength characteristics; however, the results are well described by a single curve, testifying thereby to the weak influence of the parameter $\rho_0 v_0^2/\sigma$ on the value of w_z. A change in the scale of the phenomenon (within the limits pointed out above) also does not lead to noticable deviations from the observed relationship. The consideration here refers to the case in which the residual debris beyond the perforated target is in a condensed phase, i.e., the impact speed is insufficient to vaporize the target material.

One of the basic parameters defining the overall result of a collision of a particle with a target is the diameter of the hole formed in the target. A detailed analysis of this problem was given in [13].

The authors wish to thank Academician M. A. Lavrent'ev for his interest in their work; they wish also to thank Yu. I. Fadeenko, Yu. N. Rybin, N. S. Titov, and V. P. Urushkin for useful discussions and for help with the numerous experiments.

LITERATURE CITED

1. V. M. Titov and Yu. I. Fadeenko, "Perforation by meteroid impact," Kosm. Issled., 10, No. 4, 589 (1972).
2. R. Kinslow (editor), High-Velocity Impact Phenomena, Academic Press, New York (1970).
3. V. M. Titov, Yu. I. Fadeenko, and N. S. Titova, "Shaped-charge acceleration of solid particles," Dokl. Akad. Nauk SSSR, 180, No. 5, 1051 (1968).
4. L. V. Al'tshuler, "Application of shock waves in high-pressure physics," Usp. Fiz. Nauk, 85, No. 2, 205 (1965).
5. E. N. Sher, Candidate's Dissertation, Institute of Hydrodynamics, Siberian Branch, Academy of Sciences of the USSR, Novosibirsk (1965).
6. M. A. Lavrent'ev and B. V. Shabat, Problems of Hydrodynamics and Their Mathematical Modelling [in Russian], Nauka, Moscow (1973).
7. L. A. Merzhievskii, "On the distribution of the sizes of craters formed by the residual debris cloud," in: Dynamics of a Continuous Medium [in Russian], No. 5, Inst. Gidrodinam., Sibirsk. Otd., Akad. Nauk SSSR, Novosibirsk (1970).

8. V. M. Kuznetsov, E. A. Koshelev, S. T. Safronov, and A. G. Chernikov, "Statistics of the debris fragments formed in the destruction of a solid body by an explosion," Zh. Prikl. Mekh. Tekh. Fiz., No. 2, 87 (1971).
9. L. V. Belyakov, F. F. Vitman, and N. A. Zlatin, "On the process involved in the collision of deformable bodies and a corresponding model for it," Zh. Tekh. Fiz., 33, No. 8, 990 (1963).
10. H. F. Swift, D. D. Preonas, W. C. Turpin, and J. M. Carson, "Debris clouds behind plates impacted by hypervelocity pellets," J. Spacecraft Rockets, 7, No. 3, 313 (1970).
11. F. F. Vitman and N. A. Zlatin, "On the process involved in the collision of deformable bodies and a corresponding model for it," Zh. Tekh. Fiz., 33, No. 8, 982 (1963).
12. R. W. Watson, H. R. Becker, and F. C. Gibson, "Thin plate perforation studies with projectiles in the velocity range from 2 to 5 km/sec," in: Proceedings of the Sixth Hypervelocity Impact Symposium, Vol. 3, Part 1, Cleveland (1963), p. 207.
13. L. A. Merzhievskii and Yu. I. Fadeenko, "Fracture of a fluid-filled thin-walled pipe by meteoroid impacts," Kosm. Issled., 11, No. 6, 944 (1973).